

# EUROPEAN OPTICAL NETWORK – ORBIT DETERMINATION OF RESIDENT SPACE OBJECTS

Cezary Migaszewski<sup>(1)</sup>, Stefania Wolf<sup>(1)</sup>, Piotr Stettner<sup>(1)</sup>, Piotr Wiśniewski<sup>(1)</sup>, EON Project Team<sup>(1)</sup>, Adrian Diez Martin<sup>(2)</sup>, Óscar Rodriguez Fernandez<sup>(2)</sup>, Daniel Lück<sup>(2)</sup>, and OKAPI:Orbits Team<sup>(2)</sup>

<sup>(1)</sup>Sybilla Technologies, Toruńska 59/4, 85-023 Bydgoszcz, Poland; Email: [cezary.migaszewski@sybillatechnologies.com](mailto:cezary.migaszewski@sybillatechnologies.com)

<sup>(2)</sup>OKAPI:Orbits GmbH, Rebenring 33, 38106 Braunschweig, Germany; Email: [daniel@okapiorbits.com](mailto:daniel@okapiorbits.com)

## ABSTRACT

In this contribution, we present the current capabilities of the European Optical Network (EON) in orbit determination (OD) of resident space objects (RSOs) based on astrometric observations performed with both static and tracking optical sensors. The OD precision will be demonstrated on example RSOs in the LEO, MEO and GEO orbital regimes (Low, Medium and Geostationary Earth Orbits).

The EON project is conducted as part of the European Space Agency's Space Safety Programme. It is designed to automatically observe and analyse RSOs, both active and space debris. One of its goals is to determine RSOs orbits, to build catalogues as well as to predict and avoid possible collisions and plan manoeuvres.

The network consists of static and tracking optical sensors distributed all over the globe. The static Constellation sensors (CONST) are designed mainly to monitor the GEO region, while the Panoptes (PAN) and Hydra sensors are fully controllable and can track objects in all the orbital regimes.

The sensors produce Tracking Data Messages (TDMs), which are then used to determine the orbits. The OD process can be performed on TDMs collected on one or more sensors. To illustrate the OD precision, the results are compared with precise ephemerides (SP3/CPF) and the accuracy are studied as a function of the temporal distribution of the observations as well as the orbital regime.

Keywords: Resident Space Objects; optical sensors; orbit determination.

## 1. DESCRIPTION OF THE NETWORK

The European Optical Network project was described in one of our previous works [2]. The network consists of optical telescopes (sensors) located in European Union (Poland, Spain, Hungary, Cyprus), USA, Australia, New

Zealand and South Korea. Their number increases and new sensors are being deployed. In this contribution, we will focus on the current state and capabilities of the network with six Panoptes sensors, five Constellation sensors as well as one Hydra sensor, which is a fully controllable sensor with 6 tubes on a single mount (see Figure 1 for photographs of example sensors). The telescopes are placed in 8 different locations (see Figure 2).

### 1.1. Sensors' characteristics

The sensors can be divided into two main groups, static and movable. A static sensor is pointed at a chosen place on the sky and does not change its position. It cannot track the object. It is mainly designed to observe GEO objects. A static sensor can be a single instrument, like CONST-005 (see the top-left panel of Figure 1) or be



Figure 1. Example EON sensors: CONST-005, CONST-H01, Panoptes-12 and HYDRA-02.

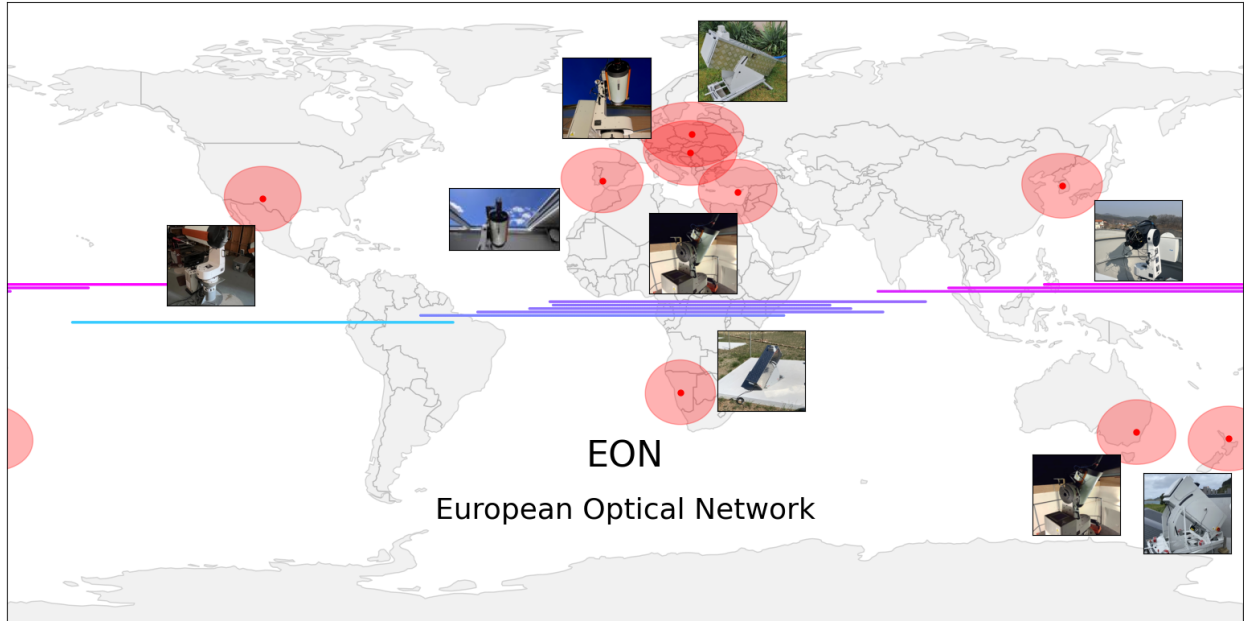


Figure 2. Locations of the EON sensors. Red areas indicate coverage of the sky for the orbit height of 500 km visible from given locations, assuming the objects are observed at elevation greater than 20 degrees. Colour horizontal lines illustrate the range of GEO belt observable from subsequent stations.

mounted on a rack, like CONST-H01 A to F sensors (see the bottom-left panel Figure 1). Each of the sensors can be pointed at a different sky position, but once they are pointed, they do not change their positions. The static sensors are the Celestron RASA8 tubes (8-inch Rowe-Ackermann Schmidt Astrograph) with QHY163M cameras with an electronic rolling shutter.

The other group of sensors are the movable ones, like Panoptes-12 (see the top-right panel of Figure 1). This sensor is a 35-cm telescope (PlaneWave DeltaRho 350) with QHY4040 camera with an electronic rolling shutter. Other Panoptes sensors are 11-inch telescopes (RASA11) with QHY600M PRO cameras. Each sensor of this type can trace the observed object, from slowly moving GEO to fast LEO objects.

Movable telescopes can be mounted in a group on a single mount (HYDRA-02) and observe the same objects in different filters (see the bottom-right panel of Figure 1). The HYDRA sensors are the RASA8 optical tubes with QHY163M cameras.

The number of sensors constituting the network increases in time as deployment and calibration of new telescopes is ongoing. The current list of sensors is given in Table 1. The list includes four new sensors deployed on March 2025 (marked with asterisks).

## 1.2. Geographical distribution

The sensors' geographical distribution is illustrated in Figure 2. While Europe is still the most densely covered

part of the world, there is at least one EON sensor on each continent (apart from Antarctica). Most of the sensors are located on the northern hemisphere. However, after adding two new sensor on the southern hemisphere there are five southern-hemisphere sensors in EON. The distribution in longitudes is sufficient to cover the GEO belt. The horizontal lines of different colours illustrate the range of the belt observable from each station above 20 degrees in altitude.

Full sky coverage of LEOs is more difficult to achieve. Red areas in Figure 2 show the sky areas at the 500-km height observable from a given site (altitudes greater than 20 degrees are assumed). Only small fraction of the sky is

Table 1. List of EON sensors as of February 2025.

Sensor name	Sensor type	Aperture (cm)	Site
Panoptes-2	movable	28	Spain
Panoptes-5	movable	28	Cyprus
Panoptes-6	movable	28	Australia
Panoptes-8	movable	28	Hungary
Panoptes-9	movable	28	USA
Panoptes-12	movable	35	South Korea
CONST-002	static	20	Namibia
CONST-003	static	20	Poland
CONST-005	static	20	New Zealand
CONST-H01(A-G)	static	20	Spain
HYDRA-02(A-F)	movable	20	Spain

available for observation. Naturally, LEO objects of typical orbital periods of 1.5 hour make 15 revolutions within 24 hours and pass above different geographical locations. On the other hand, they are illuminated and observable from a given place during daytime only for a fraction of the 24-hour time interval. It is then crucial to have dense geographical coverage of the network.

Naturally, for higher LEOs (up to 2000 km) the sky coverage is better and for MEOs the network can observe each object within 24 hours.

## 2. OBSERVATIONS

The observations are performed and processed with a help of Sybilla Technologies software, i.e., ABOT (Astronomical Robot) and Astrodrive.io [5] are used to plan and perform the observations, while collected FITS frames are processed with a help of Astrometry24.NET (A24N) [4]. Resulting TDMs contain astrometric ICRF (International Celestial Reference Frame) positions of RSOs and their magnitudes. TDMs can be used to determine orbits, which is done with the help of the Orbit Determination capabilities of the OKAPI:Orbits Aether platform. More information on the tool and its usage within the EON project is provided in [3]. Resulting orbits can be then compared to precise ephemeris, like SP3 (The Extended Standard Product 3 Orbit Format) or CPF (Consolidated Prediction Format), to study their accuracy.

### 2.1. Calibration

Each sensor must be calibrated before its TDMs can be used to determine the orbit. For a group of TDMs delivered by a given sensor, the astrometric positions (Right Ascension, R.A., and declination, Dec.) are compared to the positions stemming from ephemeris (SP3 or CPF). Apart from the geographical position of the sensor, i.e., latitude, longitude and altitude, which are found basing on GPS localisation, two parameters need to be calibrated, i.e., time bias and line period.

The time bias is a difference between actual time of exposure and the time provided by the camera. While time is synchronised by the GPS antenna connected to the sensor, there is always room for small difference due to system delays or other unrecognised effects. The time bias of our sensors is typically of the order of a few milliseconds.

Figure 3 illustrates the residual R.A. and Dec. for a series of astrometric measurements collected on Panoptes-12 over the second half of February 2025. More than 50,000 observations of GNSS (Global Navigation Satellite System) objects were collected. The observations were compared to SP3 ephemerides. The time bias is very close to

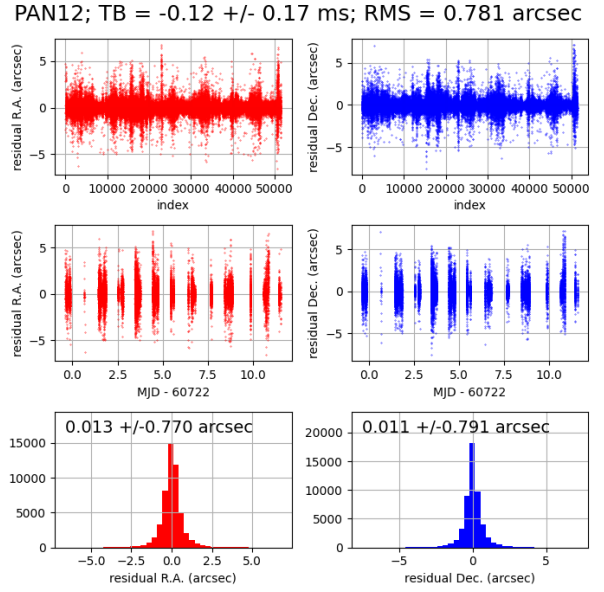


Figure 3. SP3 calibration of PAN12 on MEO objects.

0, the residuals histograms are well centred at 0 with the standard deviation of less than 0.8 arcsec.

The orbit determination of LEO objects requires a better time bias precision than derived on MEO data. Therefore, the sensors are calibrated based on LEO objects observations as well. Figure 4 illustrates the calibration results of Panoptes-2 on five LEO objects, for which SP3 ephemerides are available. The data were collected over three months, between November 2024 and February 2025. The time bias is low (-13.6 ms) and stable over this period. The RMS of the residuals is around 2 arcsec,

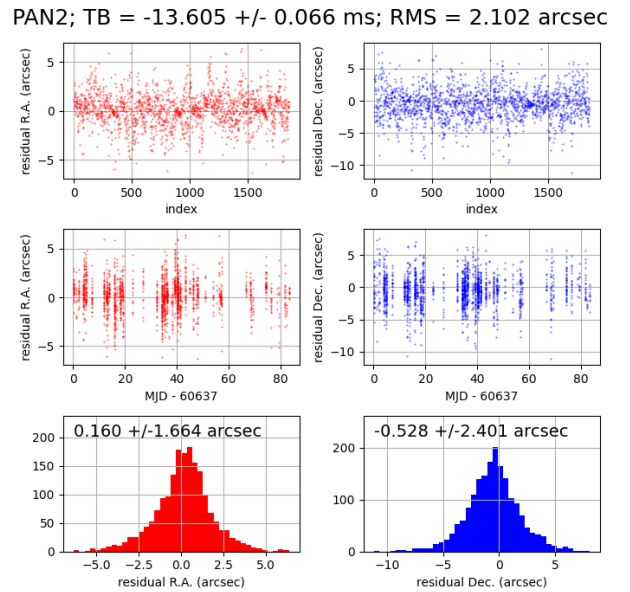


Figure 4. SP3 calibration of PAN2 on LEO objects.

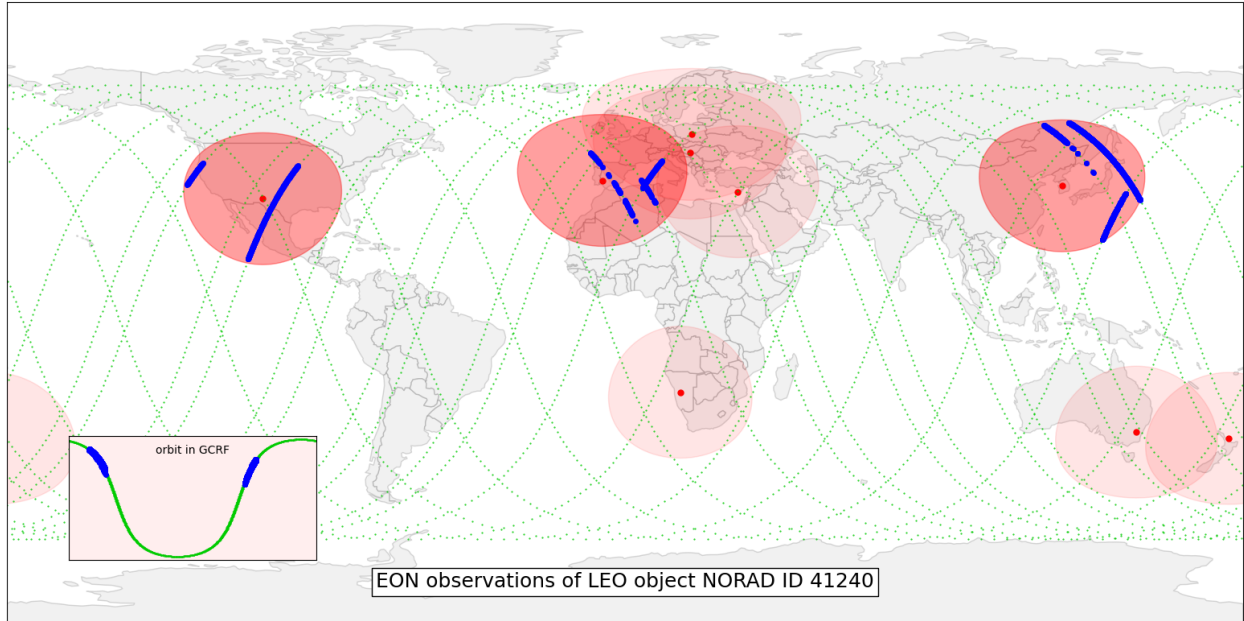


Figure 5. Observations of LEO object (NORAD ID 41240) from EON. Darker red areas indicate the stations from which the observations were made. The areas indicate observable parts of the sky from each location, assuming observations above 20 degrees in altitude and the orbit height of 1350 km. The green dots denote the ground track of the object, while blue bigger dots indicate the observed positions. A miniature plot inside illustrates the orbital coverage by the observations.

which translates to around 5 metres for a 500-km orbit and 20 metres for a 2000-km orbit.

The second parameter which must be calibrated is the line period. It characterises the rolling shutter [1], defining the time interval between activating of two subsequent rows of a camera image chip during the exposure. It is typically of the order of tens of microseconds but can be even more than a hundred microseconds. It translates to a time difference between the first and the last rows of a hundred milliseconds up to a second. The parameter is particularly important for the Constellation sensors, which observe fixed fields of the sky. The objects traversing the Field of View (FoV) are registered at different positions on the image chip, i.e., at different epoch. Moreover, the rolling shutter effect distorts the reference stellar field and therefore affects the astrometric solution of a given frame.

### 3. ORBIT DETERMINATION

Once TDMs are collected for a given object, they are used to determine the orbit using OKAPI:Orbits' Aether Platform. The tool uses their Neptune orbit propagator, which accounts for the gravitational interaction of the object with the Earth, Moon and Sun, the geopotential is modelled up to a defined degree, including the ocean and solid tides. Apart from gravity, the RSO interacts with the atmosphere as well as the solar radiation.

The aim is to find such initial condition (position and ve-

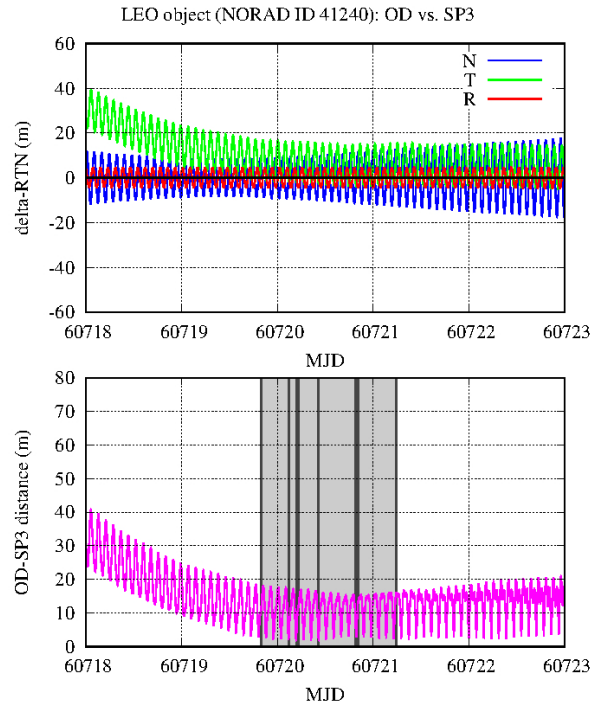


Figure 6. LEO orbit determination results. The difference between the derived orbit and the SP3 ephemeris is shown in RTN components (top) and the distance between the orbits (bottom).

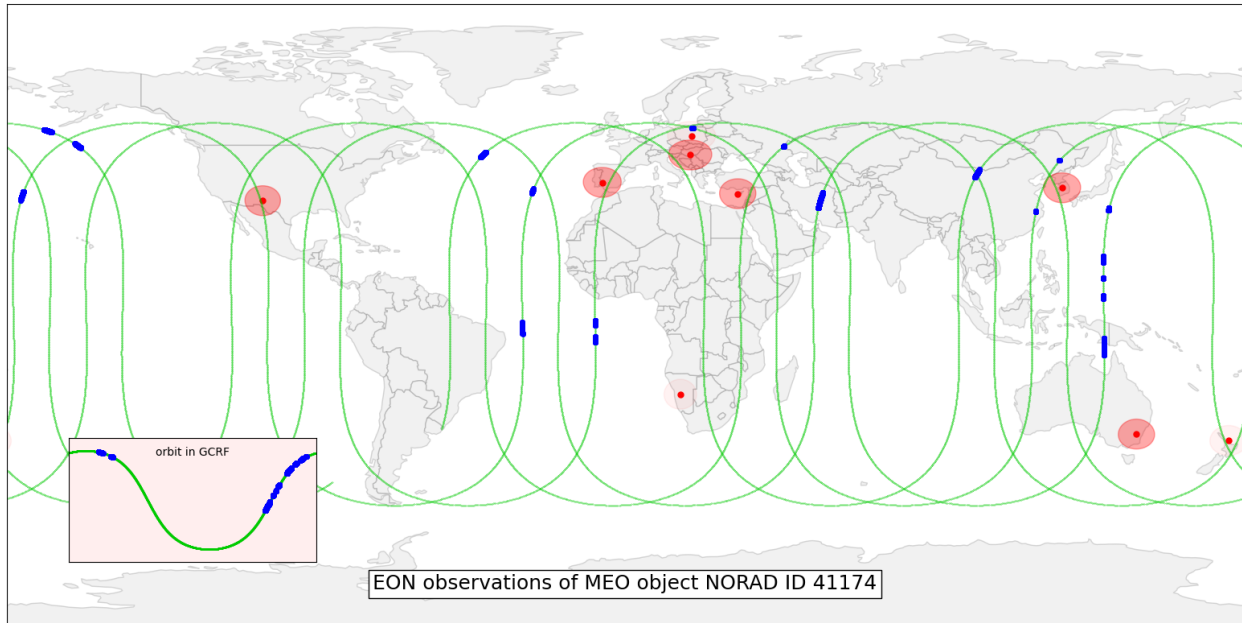


Figure 7. Observations of MEO object (NORAD ID 41174) from EON presented in a similar manner as in Figure 5. The sizes of the red areas are not related to the observable parts of the sky, since they are too big for the MEO orbit.

locity of the object in the initial epoch) which minimises the RMS (Root Mean Square). The iterative procedure starts from position and velocity found basing on the object's TLE (Two-Line Element set) by using the SGP4 (Simplified General Perturbations) model. The mass and the radar cross-section of the object is taken from available catalogue data. The OD tool can also adjust the drag coefficient as well as the reflectivity coefficient.

As a result, the best-fitting initial condition is obtained, which then can be used to propagate the orbit forwards and backwards. To study the precision of so determined orbit, it is compared to SP3 or CPF ephemerides.

### 3.1. Low Earth Orbits

We start the analysis from a LEO object of NORAD ID 41240 (Jason 3). The orbit height is  $\sim 1340$  km, while the inclination is  $\sim 66$  degrees. The ground-track of the object is illustrated in Figure 5. The object was observed in the mid-February by three sensors, i.e., PAN9, PAN2 and PAN12. The red area denotes parts of the sky seen from each location projected on the orbit height of 1340 km. The blue dots mark the places of observations. In total eight passes of the object were registered. The orbit coverage can be seen at a smaller plot inside Figure 5. The orbit is covered only partially, which results from the fact that the object was observed only from the northern hemisphere.

The precision of the orbit determination can be inspected in Figure 6. The top plot shows the difference between the determined orbit and SP3 in each component (radial,

transversal and normal). The bottom plot shows the distance between the orbit and the reference SP3 orbit. Grey area in the bottom plot indicates the observing window, while vertical lines point subsequent epochs of observa-

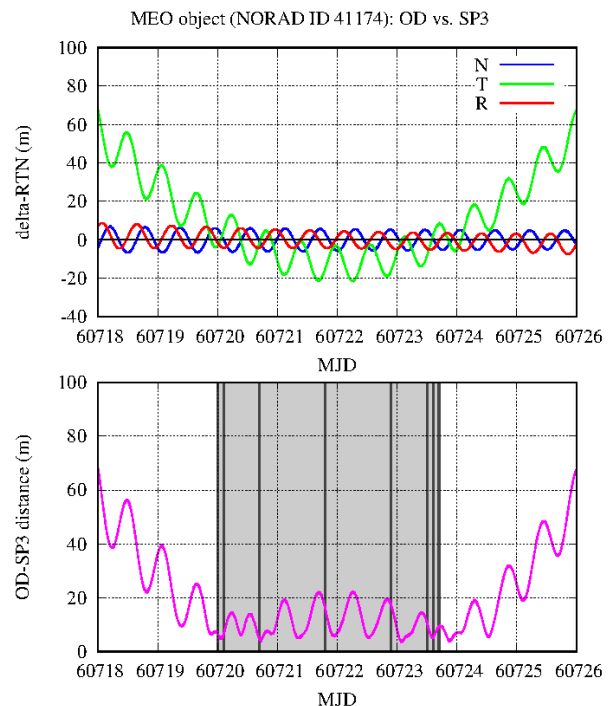


Figure 8. MEO orbit determination results shown in the same manner as in Figure 6. The SP3 ephemeris is used for a comparison.

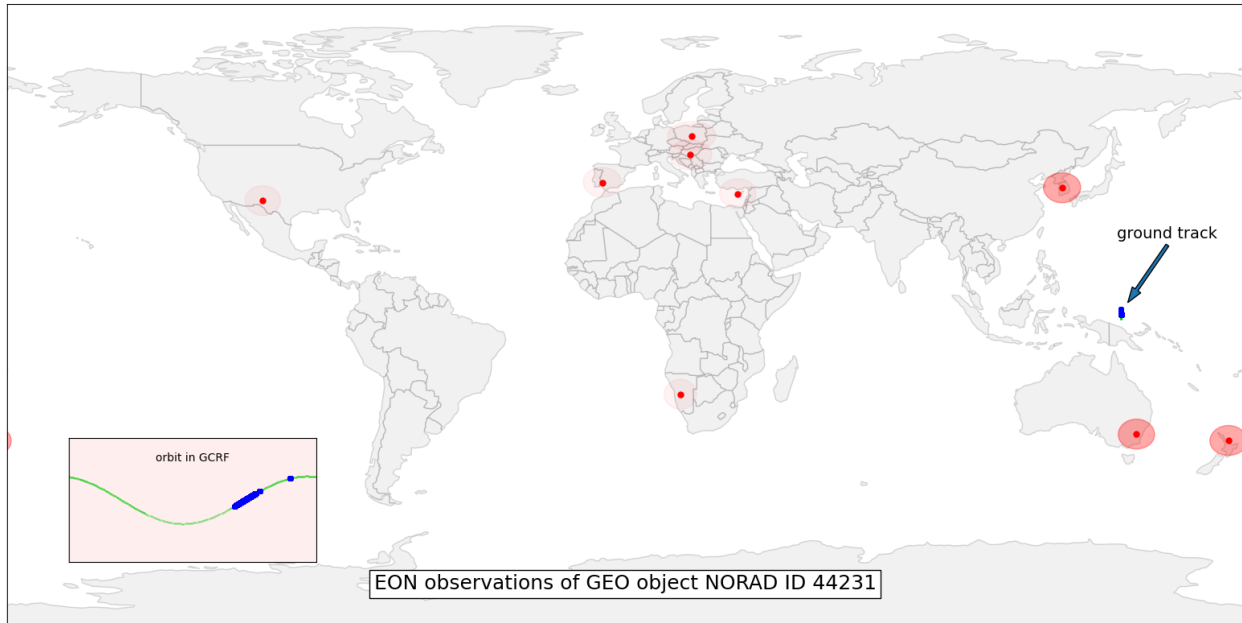


Figure 9. Observations of GEO object (NORAD ID 44231) from EON presented in a similar manner as in Figure 7. The observed object's ground track is limited to a small region and is marked with an arrow.

tions. The precision of the orbit within the observing window is kept at a level of  $\sim 20$  m, while the determined orbit slowly deviates from SP3 outside the window.

### 3.2. Medium Earth Orbits

The second example is a MEO object of NORAD ID 41174 (Galileo 12). Its orbit inclination is 56 degrees and the orbital period 845 minutes. Galileo satellites are easy to observe, and six sensors delivered TDMs for this object. Its ground-track is presented in Figure 7 and the stations from which it was observed are marked with darker red areas. The blue dots indicate observed positions of the satellite. The orbital coverage is better than for the previous LEO objects, but still more observations in the southern part of the orbit would be beneficial.

The precision of the determined orbit is studied by comparing it with the SP3 ephemeris. The results are illustrated in Figure 8. Within the observing window the orbit differs from the reference one not more than 20 metres. However, when the epochs of observations (black vertical lines in the bottom plot) are considered, the precision can go down below 10 m. Arcs of the orbit not covered by the observations are modelled with less precision. The orbit is least precise in the transversal direction, in which it slowly deviates from the reference orbit for epochs beyond the observing window.

### 3.3. Geostationary Earth Orbits

The third studied example is a geostationary RSO of NORAD ID 44231 (Beidou 2 G8). The orbit is circular and

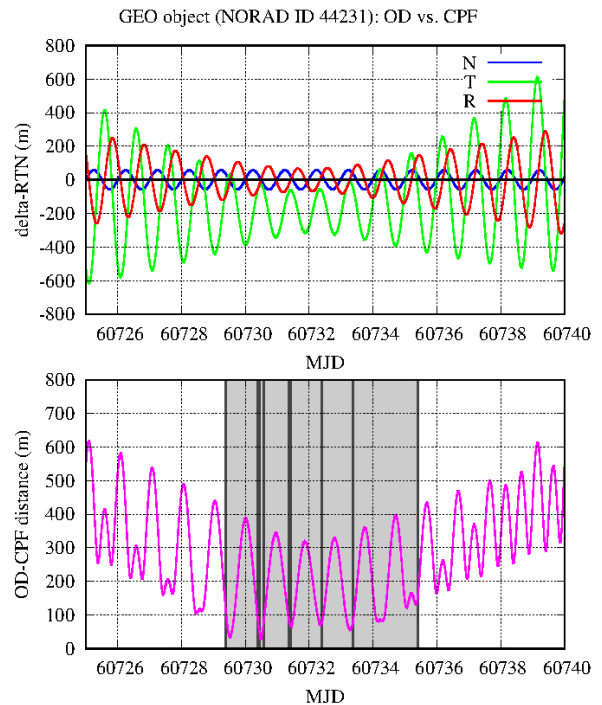


Figure 10. GEO object orbit determination results shown in the same manner as in Figure 6. The CPF ephemeris is used for a comparison.

GEO object (NORAD ID 44231): OD vs. CPF - with PAN6, PAN12 data

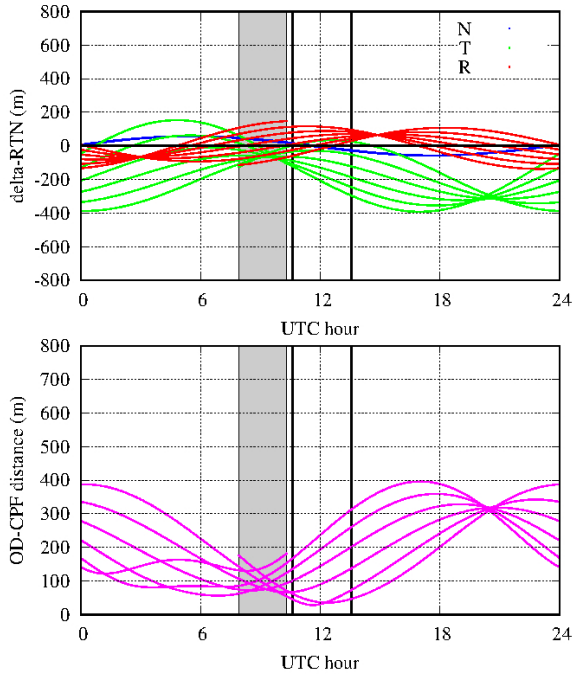


Figure 11. GEO object orbit determination precision presented as a function of the orbital phase.

has an inclination of 1.5 degree. The object was observed by three sensors (PAN12, PAN6 and CONST-005) whose positions are shown in Figure 9. All the sensors observed the object in similar epochs, however most of the data was delivered by the static sensor pointed at the GEO belt. It could observe the object for  $\sim 2.5$  hours every night, however, the object is close to one of the frame edges, and effective one can use only 1.5 – 2 hours. The two Panoptes sensors added a small fraction of the data and only one TDM was derived beyond the observing window of CONST-005.

The precision of the orbit derived on a basis of the collected TDMs is illustrated in Figure 10. The orbit is compared to a reference CPF ephemeris. Its precision of the order of a few hundred metres, however it is better in the epochs of observations. It can be better seen in a phased diagram presented in Figure 11. The difference between the orbit and CPF is phased with a 24-hour orbital period of the object. Only the epochs within the global observing window are shown (six night of observations). CONST-005 observed the object passively when it was traversing its FoV. It occurred during the same part of each night. The observing window of CONST-005 is marked with a grey area. Additionally, the Panoptes observation epochs are marked with black vertical lines. One of the epochs extends the orbital base by  $\sim 3$  hours, which will be shown later to be crucial for the orbit determination precision. The precision is kept below 400 m for all epochs and below 200 m for epochs covered by CONST-005.

GEO object (NORAD ID 44231): OD vs. CPF - only CONST-005 data

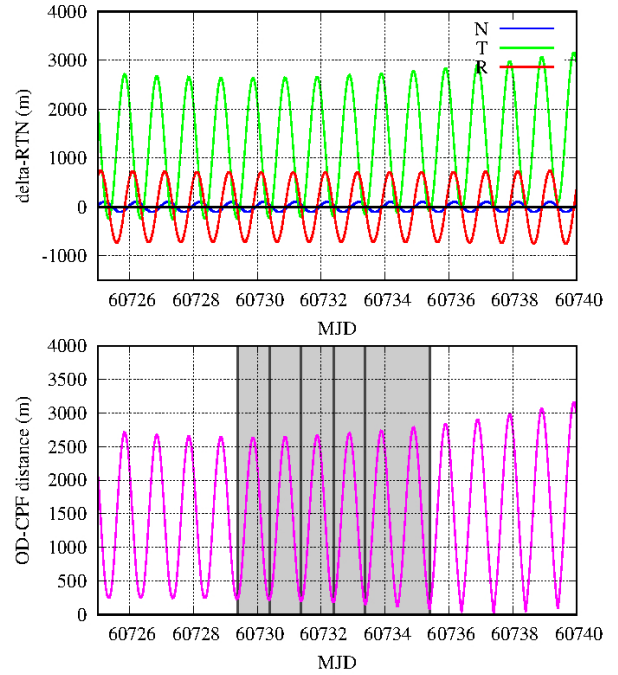


Figure 12. GEO object orbit determination of the same case as presented in Figure 10 but with PAN6 and PAN12 excluded from the sample.

### 3.4. Orbital coverage and OD precision

The observations from CONST-005 only are not enough though. If PAN6 and PAN12 data are excluded, the precision of the orbit is much worse for its side opposite to the observed one. Figure 12 and Figure 13 illustrate the results of such an experiment. The difference between the orbit and CPF is as low as it was for the full dataset in epochs of CONST-005 observations, but it grows up to three kilometres for the unobserved parts of the orbit. It is clearly seen in Figure 13. The maximal discrepancy occurs for the orbital phases opposite to the observed arc (grey area).

## 4. NETWORK DEVELOPMENT AND SUMMARY

The example presented in the previous section is an instructive illustration of how crucial a good orbital coverage for orbit determination is. To meet these requirements, we extend our network for new geographical locations. Four new sensors were deployed while writing the text of this contribution.

As a result of above mentioned as well as planned further development, the European Optical Network (EON) evolves into its commercial version, i.e., the Global European Optical Network (GEON), which is aimed at covering more evenly the globe with optical sensors. The

results presented in this contribution were obtained based on TDMs delivered by our sensors in a standard mode, i.e., the observations were not scheduled to cover the orbits of the studied objects. Only in the LEO object case the priority for this object was increased to receive more data. Still, there is a room for improvement in terms of a global observation planning for a better orbital coverage. As a result, the orbital precision should improve significantly.

## ACKNOWLEDGMENTS

The project was funded under an ESA contract No. 4000136665/21/D/MRP S2P S1-SC-09 Support of the development of sensors, joint test and operation of a European optical network, "EON".

## REFERENCES

1. A. Gurgul, M. Drzał, A. Sybilska, P. Sybilski, M. Słonina, N. Siódmiak, G. Lech, R. Ślimak, M. Pilichowski, A. Kinasz, and W. Bykowski. LightStream – enhancements to the Astrometry24.NET software for processing SST and asteroid images from CCD and CMOS. In *2nd NEO and Debris Detection Conference*, page 76, Jan. 2023.

2. A. Raiter-Smiljanic, A. Pavlovskij, M. Pietruszewska, P. Sybilski, M. Słonina, A. Gurgul, C. Kebschull, S. Flegel, D. Gondelach, K. Tsiganis, I. Gkolias, S. Kozłowski, P. Papadeas, J. Siminski, E. Cordelli, B. Jilete, T. Flohrer, and EON Team. Towards a European SST/STM system – the EON project. In *2nd NEO and Debris Detection Conference*, page 19, Jan. 2023.
3. O. Rodriguez Fernandez, D. Lück, J. Nosel, N. Eggen, R. Zabrodin, A. Diez, C. Kebschull, S. Flegel, S. Metz, J. Siminski. European Optical Network: Operational Services for GEO Operators. In *9th European Conference on Space Debris, Bonn, Germany*, Apr. 2025.
4. A. Sybilska, S. Kozłowski, P. Sybilski, R. Pawłaszek, M. Słonina, A. Gurgul, P. Konorski, M. Drzał, S. Hus, G. Lech, M. Litwicki, M. Pilichowski, R. Ślimak, U. Kolb, V. Burwitz, T. Flohrer, and Q. Funke. Astrometry24.net – precise astrometry for SST and NEO. In *1st NEO and Debris Detection Conference ESA2019*, page 10, Jan. 2019.
5. P. W. Sybilski, R. Pawłaszek, S. K. Kozłowski, M. Konacki, M. Ratajczak, and K. G. Hełminiak. Software for autonomous astronomical observatories: challenges and opportunities in the age of big data. In G. Chiozzi and N. M. Radziwill, editors, *Software and Cyberinfrastructure for Astronomy III*, volume 9152 of *Society of Photo-Optical Instrumentation Engineers (SPIE) Conference Series*, page 91521C, July 2014. doi: 10.1117/12.2055836.

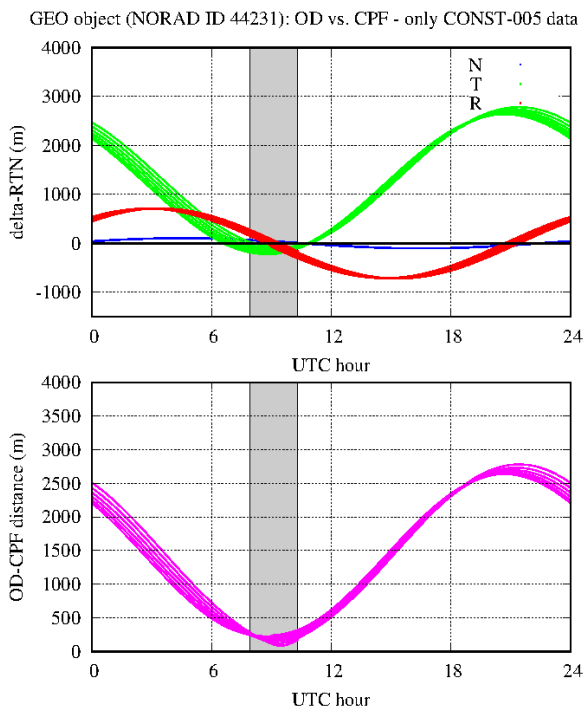


Figure 13. GEO object orbit determination precision presented as a function of the orbital phase. Only data from CONST-005 are used in the orbit determination.